FINITE ELEMENT ANALYSIS OF SALT CAVERNS EMPLOYED IN THE STRATEGIC PETROLEUM RESERVE*

DALE S. PREECE
JERRY T. FOLEY
Sandia National Laboratories
Albuquerque, New Mexico 87185

Abstract

A finite element computer program has been developed to accurately predict the creep response of rock salt. This program successfully predicted the creep response of several caverns using an approximation of the cavern geometry and material properties from the site.

The caverns at Bryan Mound, Texas have been analyzed with this program by approximating each with a two-dimensional finite element mesh. Initial leaching an3 thermal effects were treated in an approximate manner. Element removal was used to simulate the leaching which occurs when oil is withdrawn and replaced with fresh water.

Each cavern was analyzed for thirty years and an indication of the long-term stability and volume change was obtained. This information will be used to formulate operating procedures for the cavern.

*This work was performed at Sandia National Laboratories and was supported by the U.S. Department of Energy under contract number DE-AC04-76DP00789 for the U.S. Department of Energy.

INTRODUCTION

The U.S. Strategic Petroleum Reserves (SPR) is a National Program devoted to reducing America's dependence on imported oil. The program calls for storage of approximately 750 million barrels of crude oil or more. It was determined to be most economical to store the majority of this petroleum in salt caverns leached in salt domes around the Gulf of Mexico. This allowed easy access to the shipping lanes and pipeline networks which already carried much of the flow of foreign oil into the country. The naturally occurring salt domes also provided as excellent underground storage medium which was safer and more economical than steel tanks.

Another advantage to the use of salt domes was the existence of a mine and numerous caverns which were suitable for purchase and immediate petroleum storage. The final storage volume will thus be split between an existing mine, existing caverns and newly leached caverns in five salt domes around the Gulf.

The purpose of this paper is to present results of finite element analyses of caverns at Bryan Mound, Texas which were leached by industry and then purchased for use in the SPR. These cavern analyses serve as an example of the current capabilities and methods at Sandia National Laboratories for accurately predicting the response of leached salt caverns and determining thier safety.

BRYAN MOUND SALT DOME

The Bryan Mound salt dome is located in southeastern Texas near the city of Freeport. It is approximately two miles inland from the Gulf. The sides of the dome have been explored for oil since 1901, but the amount produced has been small. The major use of the site has been production of sulphur from the caprock and brine from five leached caverns. 'These five caverns were acquired by the U.S. Department of Energy (DOE) in April 1977 for use in the SPR program. All of the caverns underwent certification studies between 1977 and 1979 and all three were deemed suitable for oil storage except cavern number 3. New wells were drilled into the caverns to meet design injection and withdrawal rates and oil injection started in October, 1977 (Hogan, 1970, pg. l-l). The five caverns at Bryan Mound were analyzed in the present study to confirm the structural safety of the caverns and to predict the volume losses from the caverns due to creep closure. Figure 1 shows a plan view of the Bryan Mound salt dome and the five existing caverns in relation to each other and the edge of the dome.

ANALYSIS APPROACH

Finite element program. The finite element method offers the flexibility to treat almost any geometry with a variety of loads. This makes it ideal for analyzing salt caverns which vary greatly in shape and reside at many different depths.

A considerable amount of development work has been done on a finite element program to predict the creep response of bedded rock salt (Key, 1980). This program was a participant in the Benchmark II exercise where a generic waste isolation drift in bedded salt was analyzed (Morgan, 1981). The program's results compared very well with results from the eight other structural codes which were exercised in the benchmark study. This program was also used to analyze existing caverns which had been instrumented to provide pressure increase or volume change data due to creep closure. The results of the analysis agreed with the field data giving confidence in future work (Preece, 1982).

Volumetric calculations. The wellhead usually provides the only access to a cavern and consequently is the only point to monitor cavern response. The typical information coming from an instrumented wellhead includes pressure increase from fluid thermal expansion and creep closure, and flow from the cavern when the wellhead is opened to reduce pressure. These two parameters provide operators with a daily cavern volume change which we will call cavern flowrate.

The finite element program computes the nodal displacements at the end of each user determined time step. The volume of the cavern at each time step is computed using the coordinates and displacements at each node on the cavern surface. The volume and time data can then be manipulated into flowrates and pressure increases. It needs to be remembered that the predicted flowrates given later in this paper were obtained in this manner and do not include the flowrate due to thermal expansion of cavern fluid.

Material properties. The program uses an elastic-plastic constitutive model and a secondary creep strain model of the form

$$\dot{e}_s = A \exp(-Q/RT)(\sigma)^n \qquad (1)$$

where

$\dot{e}_s$ = secondary effective creep strain rate

A = laboratory determined constant

Q = activation energy

R = universal gas constant

T = temperature in degrees Kelvin

σ = effective stress

n = stress exponent

The coefficients in the above equation have been determined by thorough triaxial creep testing of Bryan Mound salt to be: (Wawersik, 1980)

A = 9.51 x 10^{-17} (units in days and psf)

Q = 12.1 Kcal/mole °k

n = 3.62

The elastic properties of the salt were determined from standard trixaial creep tests to be: (Wawersik, 1980)

Youngs Modulus = 6.80 x 108 psf

poissons ratio = .33

Determininq mesh width. The program can currently analyze only two-dimensional plain strain or axisymmetric geometries and since the cavern geometries are three-dimensional, this sometimes presents difficulty. If a cylindrical cavern were surrounded by six other cylindrical caverns as shown in Figure 2, the width of the mesh shown in Figure 3 can be taken as one-half the center-to-center distance between caverns. This mesh can then be treated as axisymmetric and a reasonable two-dimensional approximation of the three-dimensional geometry has been made.

If, however, the cavern we desire to analyze is surrounded by caverns on the same level as shown in Figure 4, the geometry is impossible to represent exactly with a two-dimensional axisymmetric mesh. The approach developed is a very simple one and has been partially verified with field data. The mesh width for analyzing cavern A in Figure 4 is determined by averaging half the pillar widths to surrounding caverns. In cases where there is a 180" arc around a cavern, where no other caverns exist on the same level, we also average in the pillar distance required to simulate an infinite boundary. This distance has been determined to be approximately eight times the cavern diameter. Using this information, we can calculate the mesh width required for cavern A in figure 4 as

$$W = \frac{AB/2 + AC/2 + AD/2 + 8d}{4} + \frac{d}{2} \qquad (2)$$

The outer boundary of the mesh describing cavern A is shown in Figure 4. Comparison with limited field data has shown the method to be valid. However, more data and subsequent analysis of the data source would be helpful and is being actively pursued.

Sometimes, two caverns are close enough together to violate the recommended P/D (pillar to diameter ratio) of 1.8. In this case, an analysis is performed to determine the stability of the pillar with the mesh width being chosen as half the pillar width plus the cavern radius. This is a conservative method which implies that there are six caverns surrounding the cavern of interest, each with the same pillar width. If this cavern configuration can be shown to be stable, then the actual cavern with only one other cavern at the specified pillar width is also stable.

<u>Determining mesh height</u>. Prior to the present set of analyses, the vertical' length of the mesh was made three times the height of the cavern with the cavern situated in the middle. This-works very well with a long slender cavern, but some of the caverns at Bryan Mound are shorter and wider than normal. It was determined that there should be at least twice the widest radius of the cavern in the mesh above the cavern and preferably three times. This was determined from the state of effective stress at the top of the mesh after 60 years of

creep relief. It is desirable to have the effective stress at the top of the mesh less than ten percent of the effective stress immediately surrounding the cavern. This assures minimal interference of the top of the mesh with the cavern response. The bottom of the cavern experiences less creep relief so it was determined that one cavern radius in the mesh below the cavern is sufficient. The cavern analyses which are discussed in this report do not follow these rules strictly because the rules were made based on the discoveries of the analysis. Some analyses were redone, but some which had borderline mesh heights above the cavern were taken as they were since computer costs for each analysis are quite high.

Boundary conditions. The finite element mesh of Bryan Mound cavern one is shown in Figure 5. The boundary conditions applied to this mesh are typical of those applied to the other caverns in this report. Across the top of the mesh is placed a lithostatic pressure corresponding to its depth (1 psi per foot of depth), Inside the cavern is a brinehead pressure from the surface of the ground (0.521 psi per foot of depth). Since brinehead pressure is less than lithostatic pressure, the cavern will creep inward. The right and left side of the mesh is allowed to move vertically, but is fixed horizontally as indicated by the vertical rollers. The bottom of the mesh is allowed to move horizontally (except the corners are fixed), but is fixed vertically. The creep algorithm requires a stress state to predict the next set of creep displacements in time.

To start the algorithm correctly, an initial lithostatic stress state is computed for the entire mesh and used during the first time step.

Simulating initial cavern leaching. Each cavern starts as a borehole and gradually grows as fresh water is pumped in and brine is pumped out. The borehole disturbs the stress state very little leaving a state of lithostatic stress throughout the region where the cavern will be leached. The stress at the current cavern surface has gradually changed with time from lithostatic to brinehead as the cavern developed from a borehole to its present state. It has been determined that this leaching process must be simulated in order to accurately predict the cavern response immediately after leaching is completed. One method is to linearly reduce the pressure inside the current cavern geometry from lithostatic to brinehead over a finite period of time. Figure 6 shows the predicted flowrate from cavern one (depicted in Figure 5) for three different treatments of the initial leaching. Curve A shows the cavern response when the cavern is loaded initially with brinehead pressure inside. In this case, the effective stress around the cavern is very large initially and gradually dissipates through creep relief. Curves B and C show the cavern response when the pressure inside is reduced from lithostatic to brinehead over 300 days and 1000 days, respectively. In these cases, the initial effective stress around the cavern is zero as it would be before the cavern was leached. The effective stress increases as the inside pressure is reduced. At the time the pressure reaches brinehead, the effective stress around the cavern is at a maximum then it gradually dissipates with time to steady state effective stress. In all three cases, the steady state effective stress distribution on the mesh is essentially the same and corresponds to the steady state flowrate from about 3000 days on in Figure 6.

Simulating cavern leaching during oil withdrawal. The SPR program is designed to allow five oil withdrawals of each cavern during its thirty year life. When the oil is withdrawn, it is replaced by fresh water which leaches the cavern to a larger size. A computer program for predicting leaching was obtained by the Fluid and Thermal Sciences Department at Sandia and changed to better meet SPR needs (Saberian, 1977). This program is used to predict the new cavern size after each leaching cycle (Russo, 1981). The cavern leaching is taken into account during the finite element analysis by predefining the mesh to match the layers which will be leached as shown in Figure 7. The timing of the five withdrawals is not known and depends on the national energy situation. For analytical purposes, the withdrawals were divided evenly over the life of the SPR program (30 years), and occurred every six years. At the time the withdrawal occurs, the pressure is removed from the current surface, one layer of elements is removed and the pressure is placed on the new surface simultaneously. The flowrate from the cavern due to creep closure increases because the volume has increased. Figure 8 shows the total volume of cavern one plotted against time. Each step in the curve represents a volume increase due to leaching. After each volume increase, the cavern continues to creep inward as shown in the close-up of one leaching cycle in Figure 9.

Temperature effects. As can be seen in equation (1), the creep rate is an exponential function of temperature. The fluid going into the cavern is approximately 70°F and gradually heats to the in-situ temperature of the cavern (between 100°F and 130°F depending on depth). This has two effects, first the fluid expands as it-heats and flows from the cavern if the wellhead is open or increases the internal pressure if the wellhead is shut. Second, the fluid cools the walls of the cavern resulting in thermal contraction and temporary reduction in creep rate. The computer program has the capability to treat the thermal stress problem and also the thermal influence on creep. A thermal analysis of one cavern was performed by Tony Russo which included the initial placement of cool fluid in a cavern and subdequent injections of cool fluid for the drawdown/leaching cycles. This time dependent thermal field was included in the structural creep analysis of the cavern. The same analysis was also made without the time dependent thermal field but using a constant temperature corresponding to the average temperature of the mesh. Immediately after the first cool fluid injection, the analysis which included the thermal field had a flowrate which was 50% less than the flowrate in the constant temperature analysis. Within three or four years, however, the two flowrates were about the same.

The process of performing a thermal analysis on each cavern and transferring the data to the finite element mesh was cumbersome and time consuming. It was decided that for the present, the analyses would be performed with a constant temperature. It is felt that this gives a good representation of the cavern performance three or four years from the time of injection.

<u>Predicting salt fracture</u>, A function which conservatively predicts when rock salt will fracture or crush has been proposed by Wolfgang Wawersik (Miller, 1982, pg 36-37). This function relates confining pressure and effective creep strain and becomes positive when the potential for fracture or crushing exists.

$$\phi = 150.0\ (E - 0.023 - f(p)$$

$$f(P) = \begin{cases} 0.132 & \text{for } P \geq 1.256 \times 10^{5} \text{ psf} \\ (2.117 \times 10^{-6})\ P - (8.450 \times 10^{12}) P^{2} & \text{otherwise} \end{cases}$$

where

ϕ = fracture/crush function

$P = (\sigma_1 + \sigma_2 + \sigma_3)/3.0$ (confining pressure)

$f(P)$ = function of confining pressure

The determination of possible problem regions around a cavern is done by post-processing the finite element data to determine if the function ϕ is positive anywhere on the mesh. There is no provision for computing ϕ during the analysis and redistributing stresses when fracture occurs.

BRYAN MOUND CAVERN ONE

The well for Bryan Mound Cavern one was initially drilled in 1942. The volume of the cavern is currently 5.3 million barrels (mmb). The cavern is located well away from the edge of the dome and the caprock, but has a pillar of only 245 feet between it and cavern four. Caverns four and five are the only existing caverns that are on the same level as cavern one. Two new caverns will be leached about 800 feet from cavern one and two new caverns will be leached about 1000 feet from cavern one. These will also be on the same level as cavern one. The shape of the cavern as determined from sonar data is shown in Figure 10 (Hogan, 1980 pg. 4). The finite element model of cavern one is shown in Figure 5 and has a volume of 5.0 mmb. The volumetric response of the cavern versus time is given in Figure 8 and a summary of the flow rates immediately before each oil withdrawal is given in Table 1.

Post-processing of the fracture/crush function given earlier shows the cavern to be structurally sound and will continue as such through the first several drawdown cycles. There is the possibility of coalescence with cavern four on the second or third drawdown requiring that the growth of both caverns be monitored closely. Because of our two-dimensional approach, the present analysis will not predict the stresses or fracturing of the pillar as the two caverns approach each other. This can, however, be treated approximately by performing another analysis with a narrower mesh.

TABLE I

Cavern One Flowrates

Withdrawal Number	initial	1	2	3	4	5
Volume (x 10^7 ft^3)	2.79	3.29	3.90	4.56	5.27	6.00
Flowrate (ft^3/day)	29.7	35.1	43.5	58.7	69.8	79.9

BRYAN MOUND CAVERN TWO

The initiation well for cavern two was drilled in 1942 and the 5.5 mmb cavern shown in Figure 11 was subsequently developed. Cavern three is the only cavern (including the new caverns) on the same level as cavern two and is located 450 feet away. The cavern is well away from the edge of the dome, but is only 365 feet below the caprock. This distance has been deemed suitable by past and present finite element analyses (Hogan, 1980, pg 4). The finite element mesh, as shown in Figure 12 has a volume of 4.9 mmb. The volumetric response of the cavern versus time is given in Figure 13 and the flowrates immediately before each oil withdrawal is given 'in Table II.

Results from the fracture/crush function show this cavern to be structurally sound throughout its entire SPR life including the five drawdown cycles.

TABLE II

Cavern Two Flowrates

Withdrawal Number	initial	1	2	3	4	5
Volume (x 10^7 ft^3)	2.73	3.39	4.14	4.99	5.89	6.87
Flowrate (ft^3/day)	5.9	7.5	14.3	17.0	41.8	28.1

BRYAN MOUND CAVERN THREE

Cavern three was initiated in 1941 and currently has a volume of 6.4 mmb. This cavern was purchased for oil storage along with the rest of the caverns, but was subsequently deemed unsuitable for oil storage. Early in its testing, it appeared to have fresh water circulation and continual leaching taking place within the cavern. There are also problems with the well leaking and until both of these problems are fixed or reconciled, oil will not be stored in this cavern (Hogan, 1980, pg 5).

A finite element analysis of the cavern was carried out in the present study to confirm its structural stability over the life of the SPR program and to predict the creep closure rate of the cavern.

The cavern, shown in Figure 14, has a volume of 6.4 mmb. The cavern is relatively shallow and cavern 2 is the only other cavern on the same level. The finite element mesh which has a cavern volume of 12.76 mmb is shown in Figure 15. The mesh was made using one cross-section (which is apparently the largest) obtained from the sonar surveys. The mesh was used because showing that this larger cavern is structurally sound would also indicate the safety of the actual cavern. The fracture/crush function shows this cavern to be stable throughout the life of the SPR program. The analysis predicts a loss of approximately two percent of the original volume over sixty years. Unfortunately, there doesn't seem to be any field data to compare with.

BRYAN MOUND CAVERN FOUR

Cavern four is the second Largest cavern in the SPR program with a volume of 16.3 mmb. The well for this cavern was drilled in 1942 and gradually developed into the shape shown in Figure 16. This cavern is approximately in the center of the dome and is 1500 feet below the caprock so no edge of dome or roof thickness problems are anticipated. Caverns one and five are on the same level and relatively close (pillar thicknesses of 245 feet and 320 feet, respectively). Three of the new expansion caverns are also on the same level and within approximately 1100 feet (Hogan, 1980, pg 6). The finite element mesh shown in Figure 17 has a cavern volume of 16.9 mmb. The volumetric response of the cavern is given in Figure 18 and a summary of the flowrates from the cavern immediately before each drawdown is given in Table III.

Post-processing of the fracture/crush function indicates the present and future (after five drawdown cycles) stability of this cavern. There is the possibility of coalescence with cavern one as mentioned previously and also cavern five. The growth of these three caverns and the pillar distances between them needs to-be closely monitored.

TABLE III

Cavern Four Flowrates

Withdrawal Number	initial	1	2	3	4	5
Volume (x 10^7 ft^3)	9.22	10.63	12.17	13.86'	15.68	17.44
Flowrate (ft^3/day)	160.1	206.7	271.5	340.0	423.1	503.77

BRYAN MOUND CAVERN FIVE

Cavern five was initiated in 1957 and subsequently developed into the 33.4 mmb cavern shown in Figure 19. The cavern has an upper and lower lobe separated by what appears to be an insoluable layer (the ledge may also be the result of the leaching process rather than insolubility). This cavern is the largest in the SPR program, but since it is over 650 feet from the dome edge and 1000 feet from the caprock, no edge of dome or roof thickness problems are anticipated. Cavern four and two new expansion caverns are located on the same level as this cavern. Also included in the determination of the mesh width was the distance to the edge of the dome (Hogan, 1980 pg 6). The finite element mesh of the cavern in Figure 20 has a volume of 33.4 mmb. This mesh does not include a layer of elements for each drawdown. An attempt was made to include the layers, but the resulting mesh was so fine and had so many elements as to make the analysis overly expensive. The present mesh has one layer of elements between the original and final size. The volumetric response of the cavern is given in Figure 21 and a summary of the flowrate after each drawdown is given in Table IV.

The post-processed fracture/crush function does not indicate any stability problems of the cavern at present or in the future. As mentioned previously, there is the possibility of coalescence with cavern four and the present analysis would not predict any pillar stability problems associated with the coalescence process.

TABLE IV

Cavern Five Flowrates

Withdrawal Number	initial	1	2	3	4	5
Volume (x 10^7 ft^3)	18.0	--	--	--	--	26.3
Flowrate (ft^3/day)	448.8	--	--	--	--	849.6

SUMMARY

The methods presented in this paper for determining creep response of leached salt caverns seem to work reasonably well considering the limits of two-dimensional analysis. The volume change versus time data, which has been predicted, will be useful to cavern operators as they plan bleed down schedules, brine buffer sizes, and disposal of brine displaced from the cavern due to creep closure. The ability to predict and plan should result in a more efficient cavern operation.

BIBLIOGRAPHY

Hogan, R. G., 1980, Strategic Petroleum Reserve Geologicasl Site Characterization Report Bryan Mound Salt Dome, Sandia National Laboratories, SAND80-7111.

Key, S. W., Stone, C. M., and Krieg, R. D., 1980, A Solution Strategy for the Quasi-Static Large Deformation Inelastic Response of Axisymmetric Solids, presented at U.S. European Workshop Nonlinear Finite Element Analysis in Structural Mechanics, Ruhr-Universitat; Bochyum, W. Germany.

Miller, J. D., Stone, C. M., and Branstetter, L. J., 1982, Reference Calculations for Underground Rooms of the WIPP, Sandia National Laboratories, SAND82-1176.

Morgan, H. S., Krieg, R. D., and Matalucci, R. V., 1981, Comparative Analysis of Nine Structural Codes Used in the Second WIPP Benchmark Problem, Sandia National Laboratories, SAND81-1389.

Preece, D. S., and Stone, C. M., 1982, Verification of Finite Element Methods Used to Predict Creep Response of Leached Salt Caverns, 23rd Symposium on Rock Mechanics, Berkeley, CA.

Russo, Anthony J., 1981, A Solution Mining Code for Studying Axisymmetric Salt Cavern Formation, Sandia National Laboratories, SAND81-1231.

Saverian, A., and Podio, A. L., 1977, A Computer Model for Describing the Development of Solution-Mined Cavities, IN SITU, l(l), p. l-36.

Wawersik, W. R., Holcomb, D. J., Hannum, D. W., 1980, Quasi-Static and Creep Data for Dome Salt From Bryan Mound, Texas, Sandia National Laboratories, SAND809-1434.

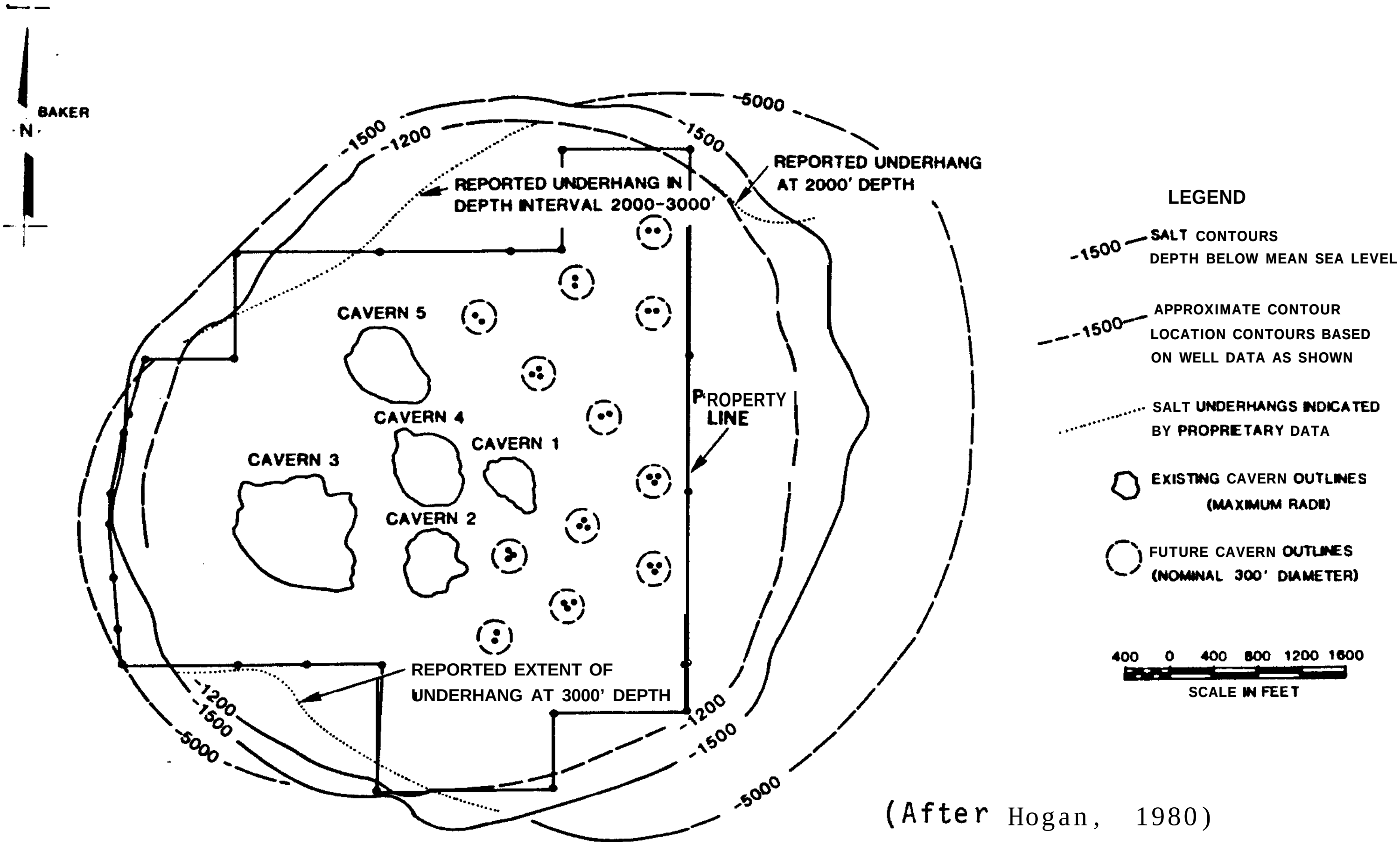

(After Hogan, 1980)

Figure 1

Plan View of Bryan Mound Salt Dome

(Being made by Tech Art)

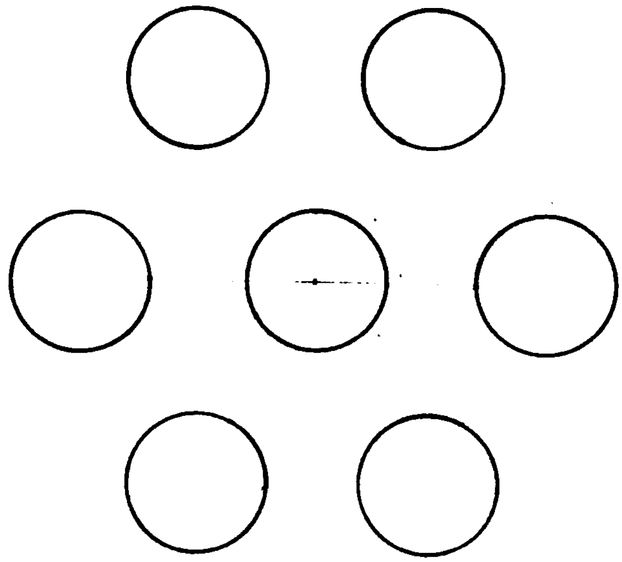

Figure 2
Top view of cylindrical cavern array

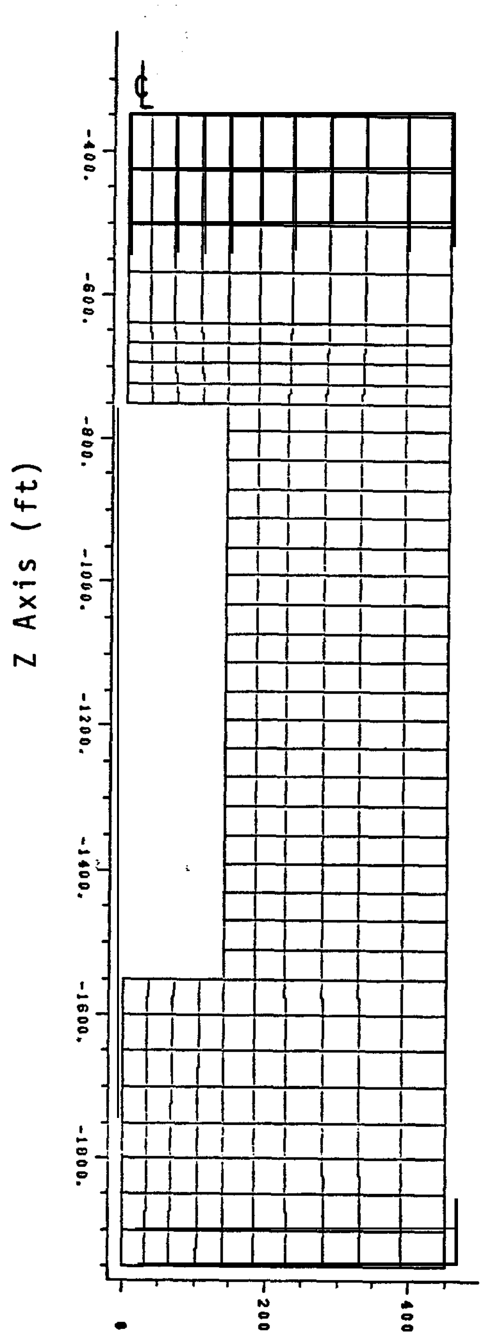

R Axis (ft)

Figure 3

Vertical Axisymmetric Finite Element Mesh
of Cylindrical Cavern

(Being made by Tech Art)

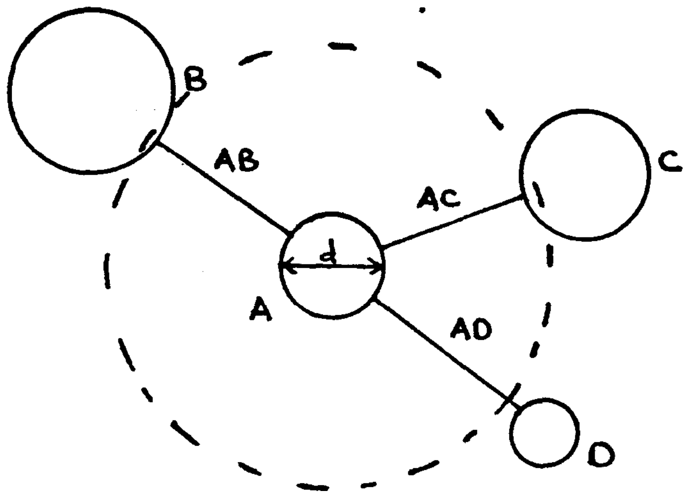

Figure 4
Top view of a typical cavern group

(Being made by Tech Art)

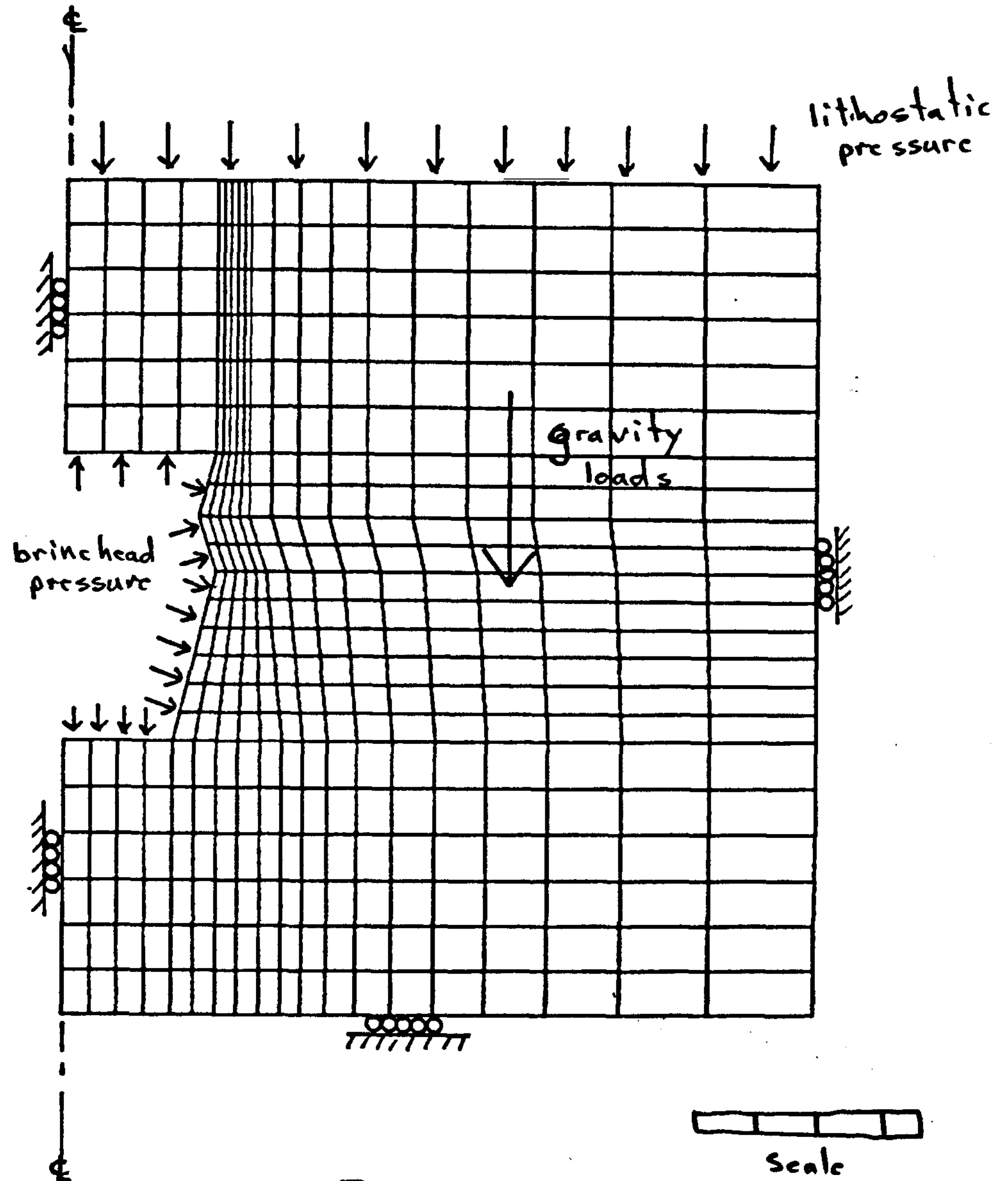

Figure 5

Axisymmetric finite element model of Bryan Mound cavern one.

(Being made by Tech Art)

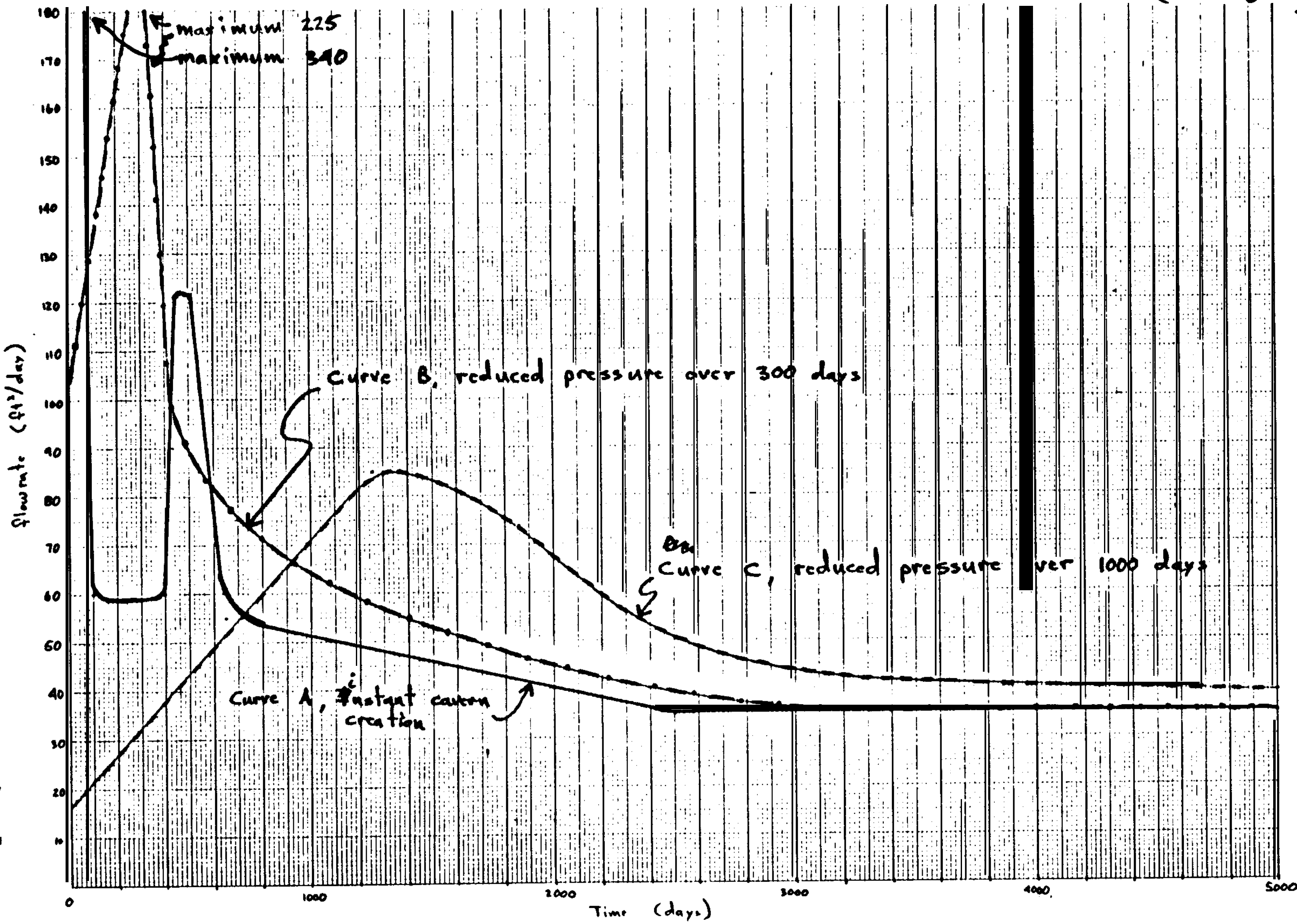

Figure 6
Flow rate versus time for three differant treatment of the initial leaching process

Being made by
Tech Art

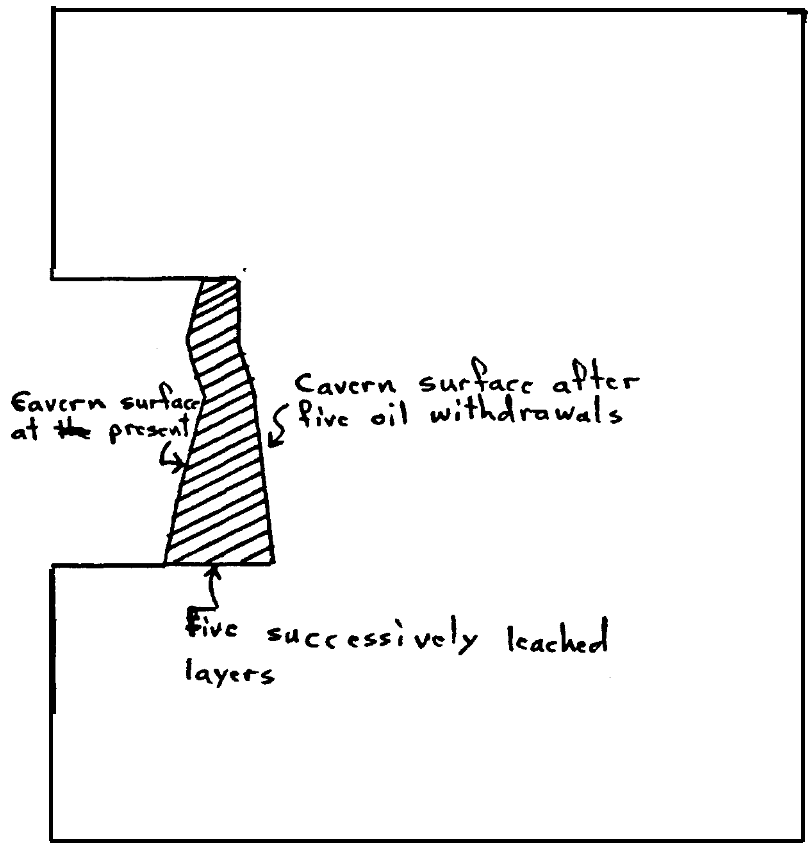

Figure 7

Bryan Mound cavern one with leached layers cross hatched

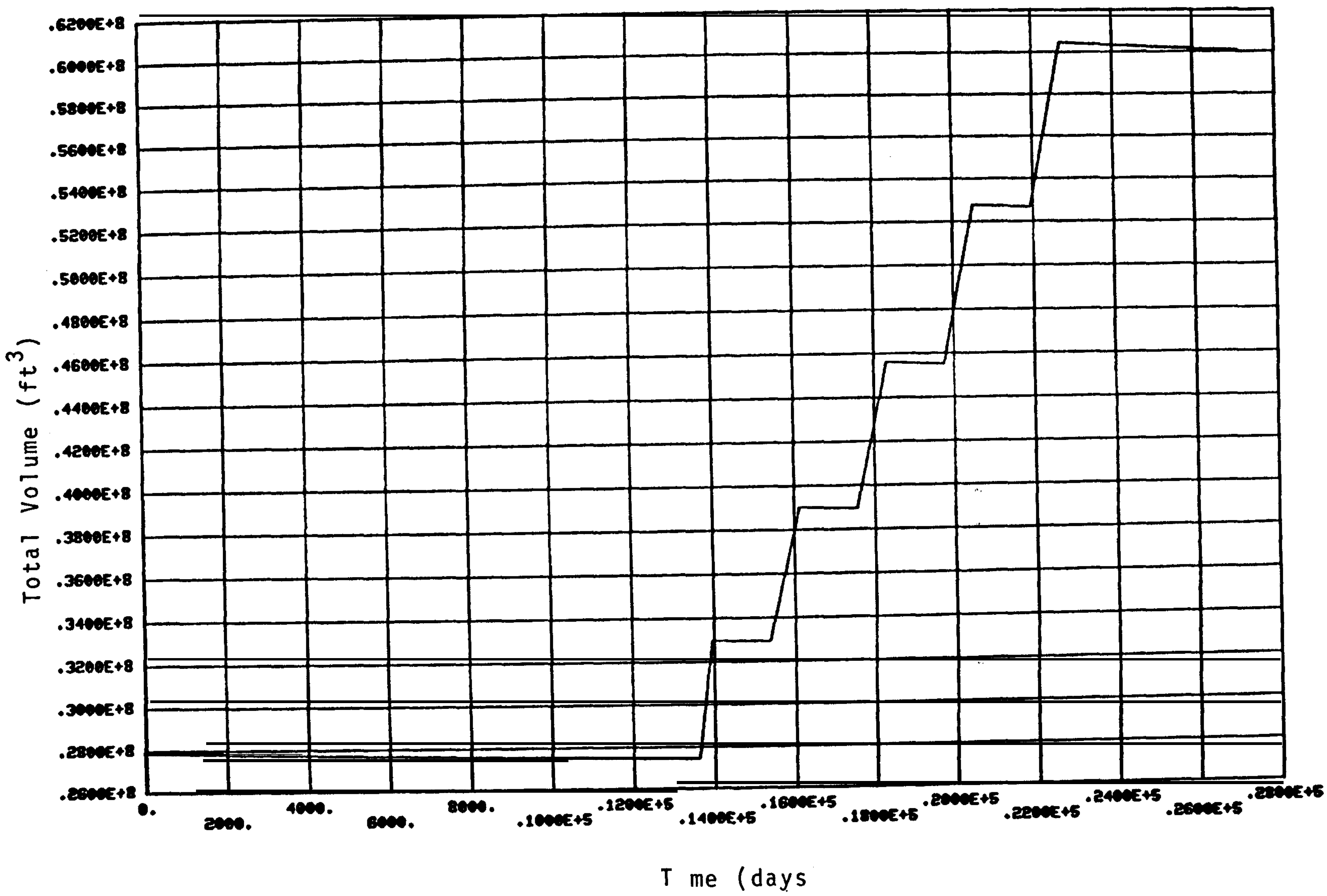

Figure 8
Volumetric Response of Cavern One

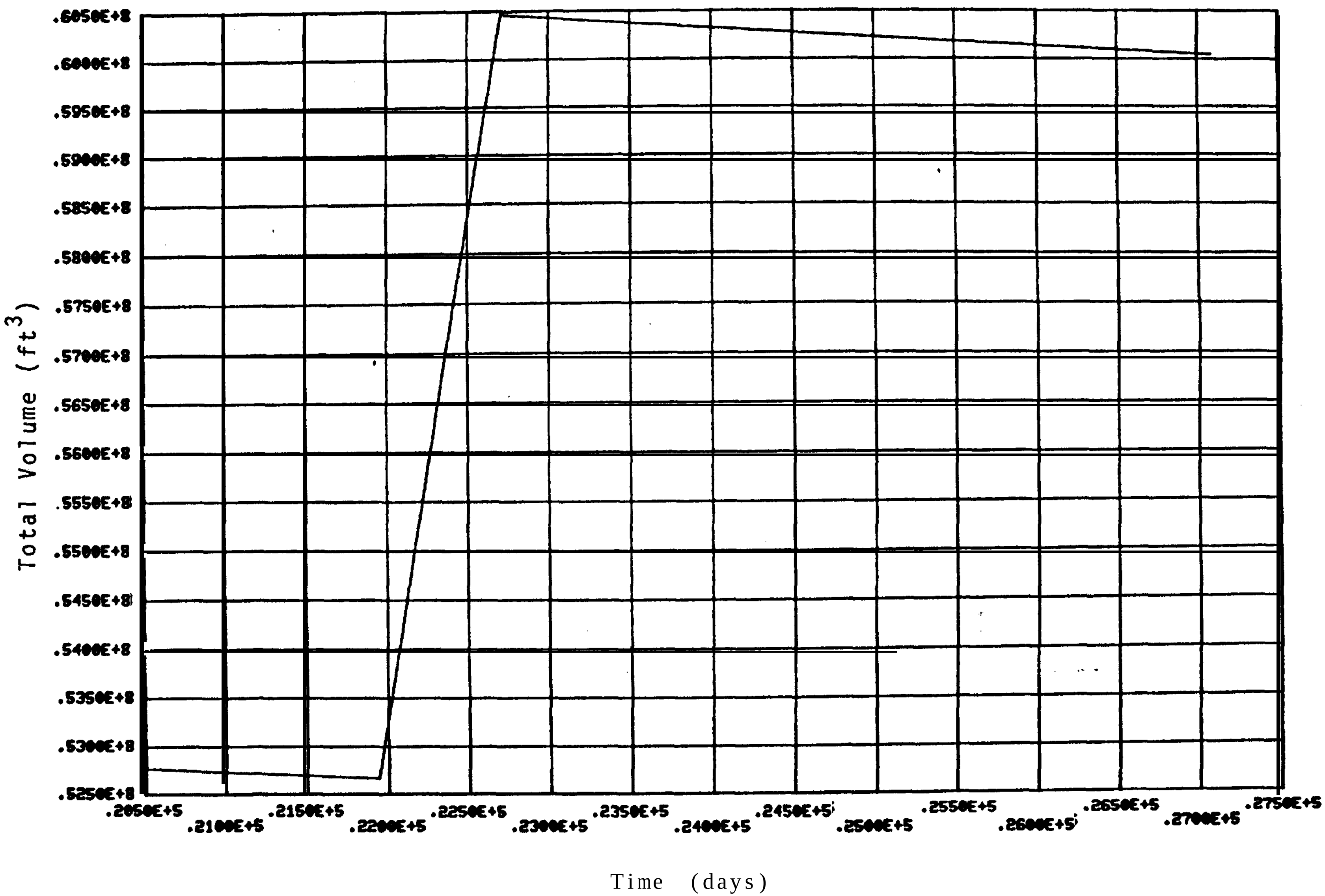

Figure 9

Final Leaching Cycle of Bryan Mound
Cavern One

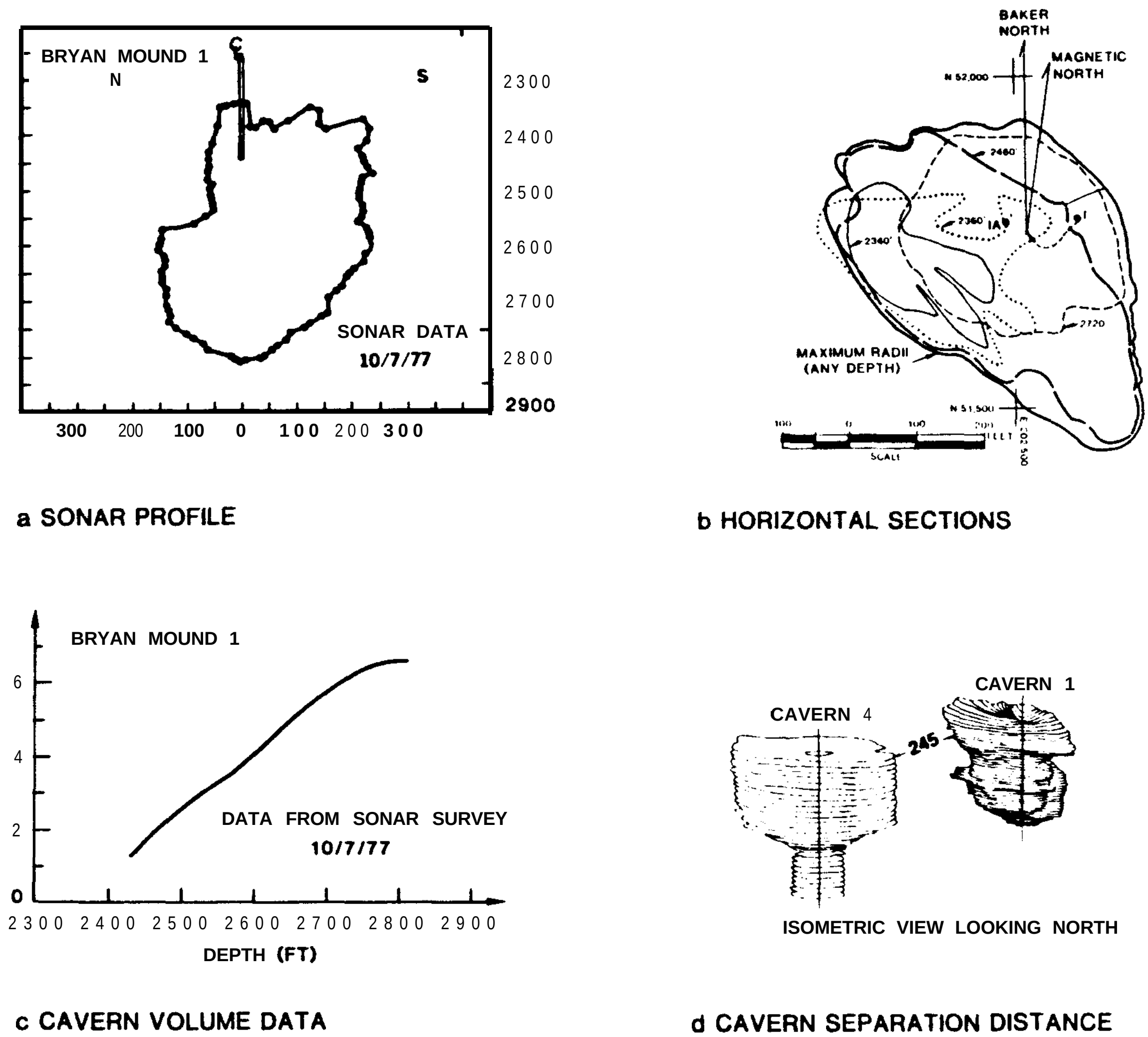

(After Hogan, 1980)

Figure 10
Bryan Mound Cavern One

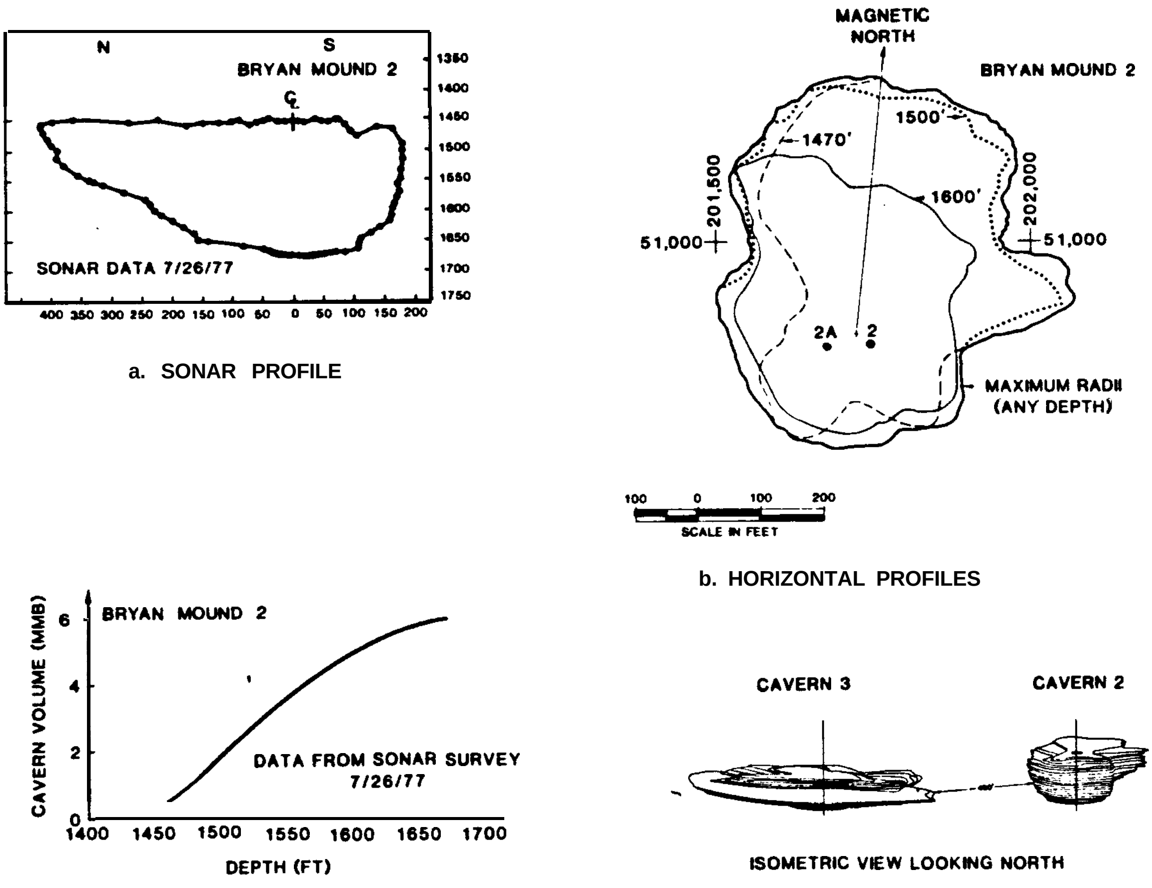

a. SONAR PROFILE

b. HORIZONTAL PROFILES

c. CAVERN VOLUME DATA

d. CAVERN SEPARATION DISTANCE

(After Hogan, 1980)

Figure 11

Bryan Mound Cavern Two

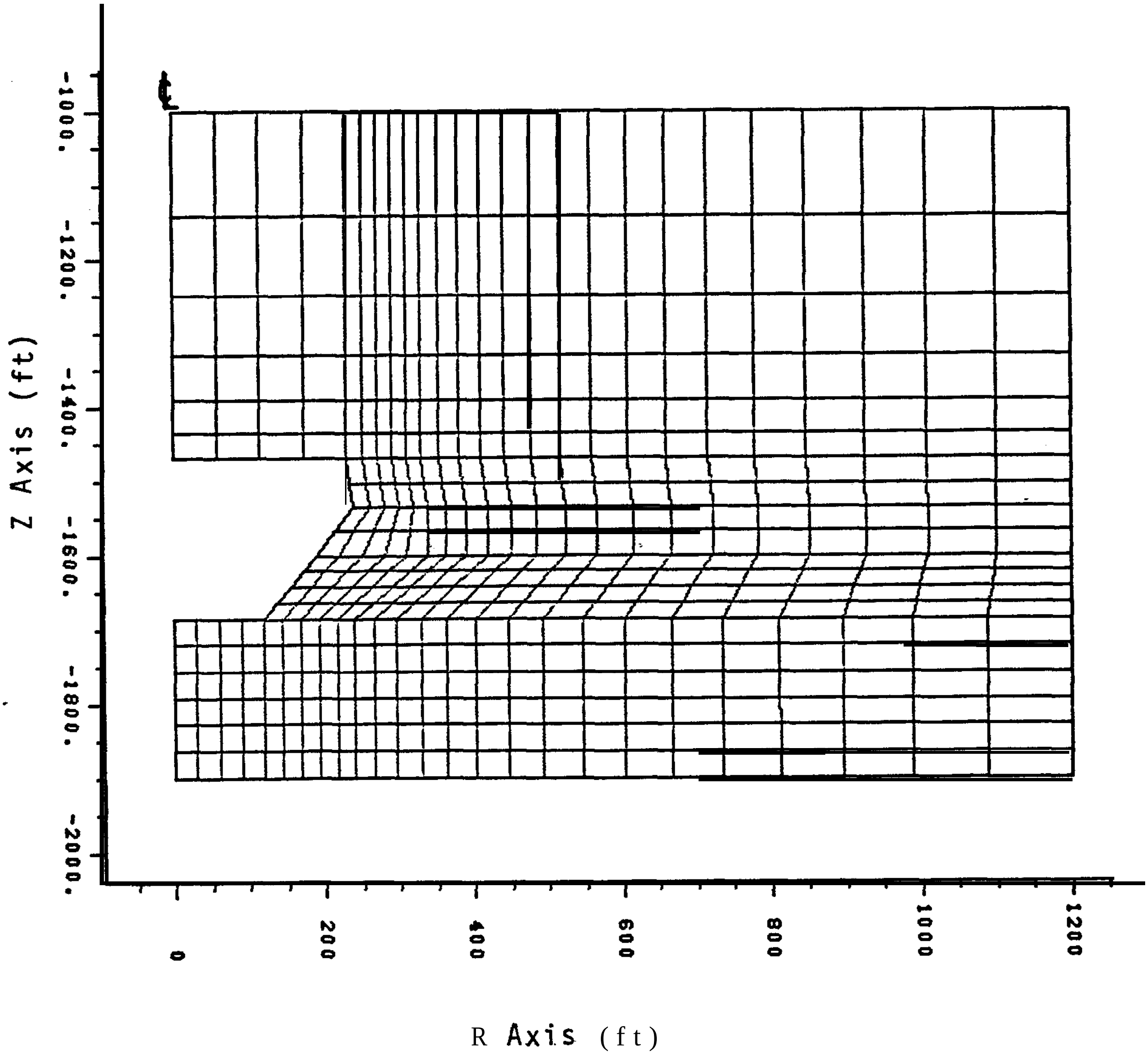

Figure 12

Axisymmetric Finite Element Mesh
of Bryan Mound Cavern Two

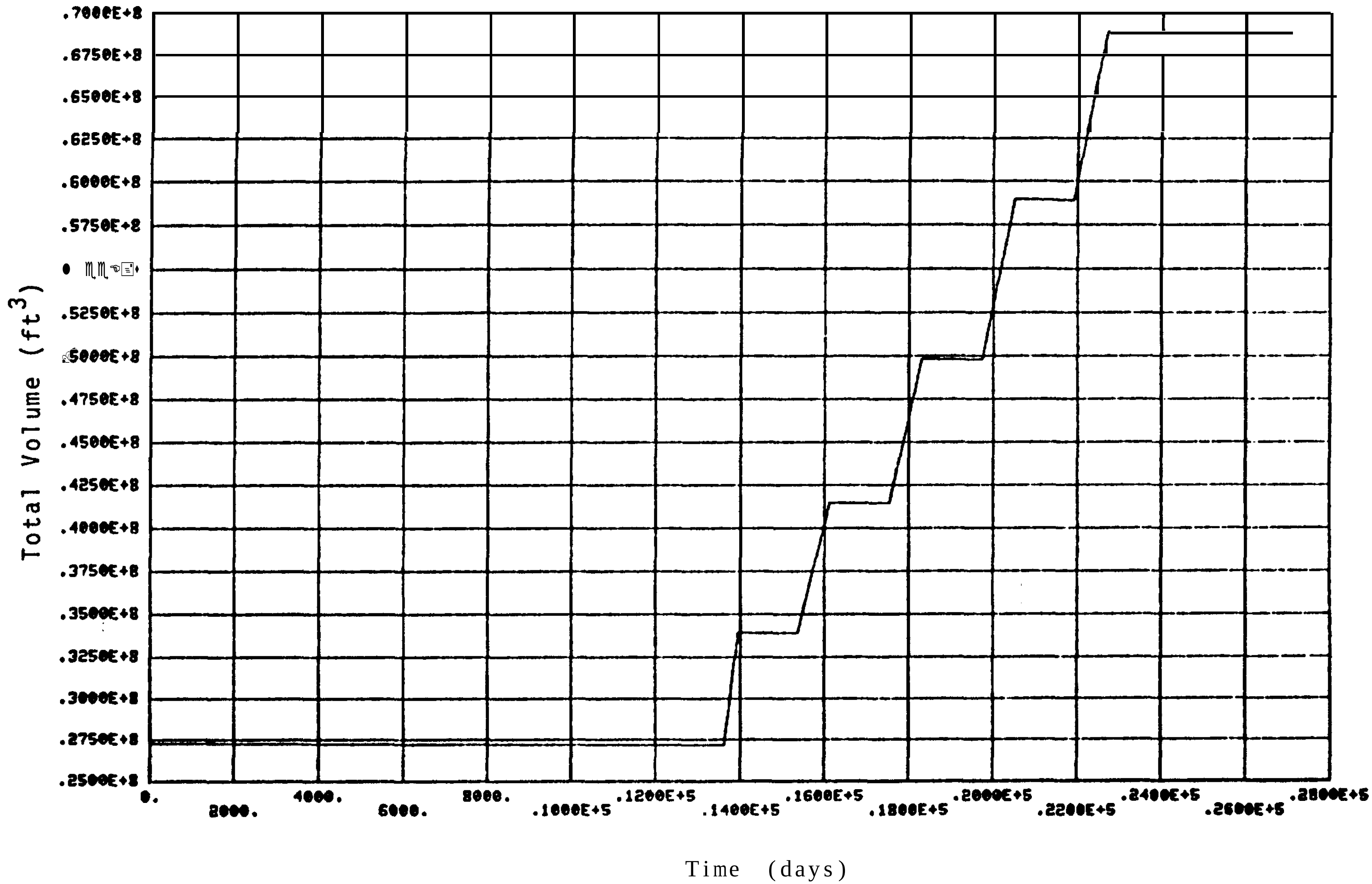

Figure 13
Volumetric Response of Cavern Two

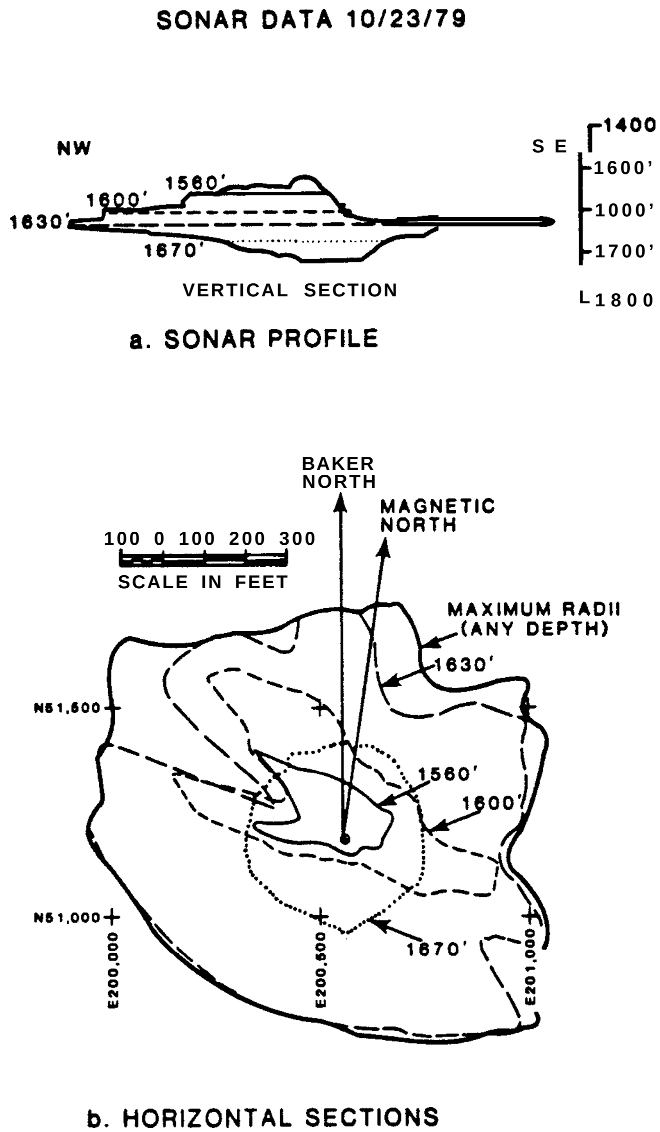

(After Hogan, 1980)

Figure 14
Bryan Mound Cavern Three

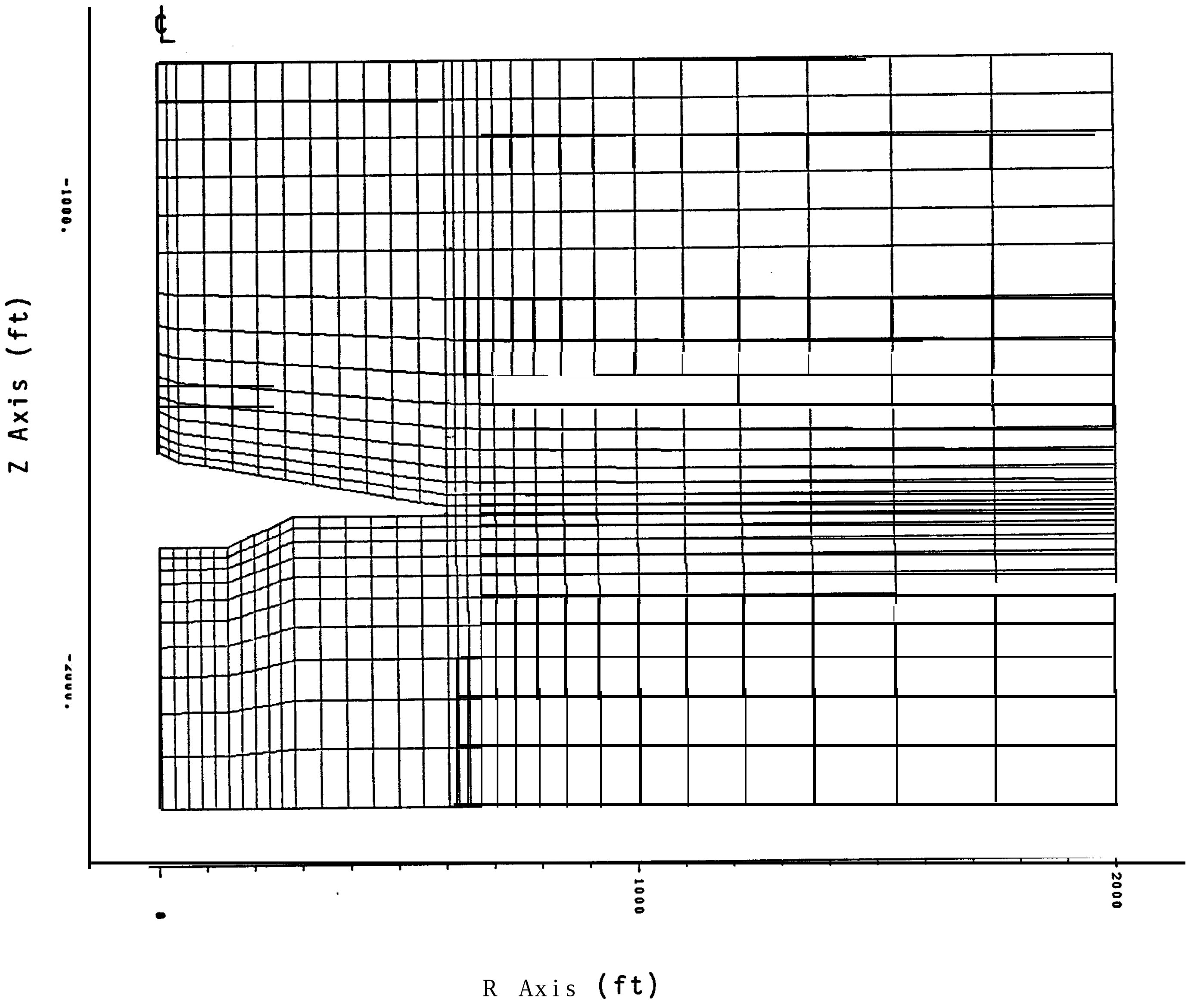

Figure 15

Axisymmetric Finite Element Mesh of Bryan Mound Three

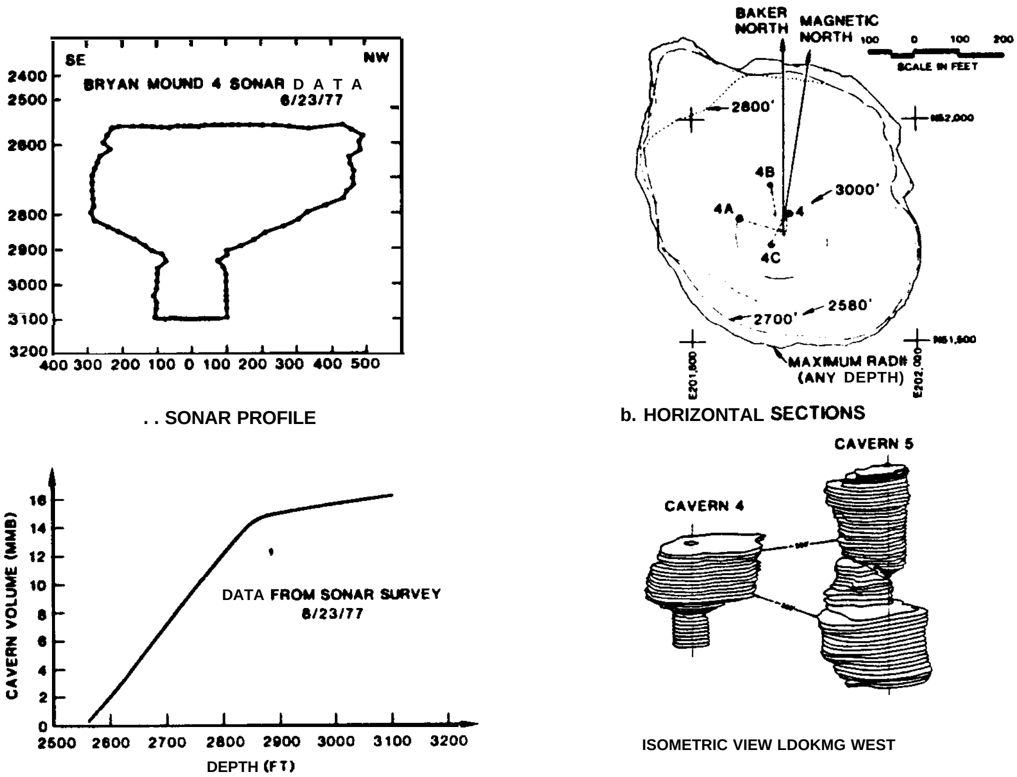

. . SONAR PROFILE

b. HORIZONTAL SECTIONS

c. CAVERN VOLUME DATA

d. CAVERN SEPARATION DISTANCE

(After Hogan, 1980)

Figure 16

Bryan Mound Cavern Four

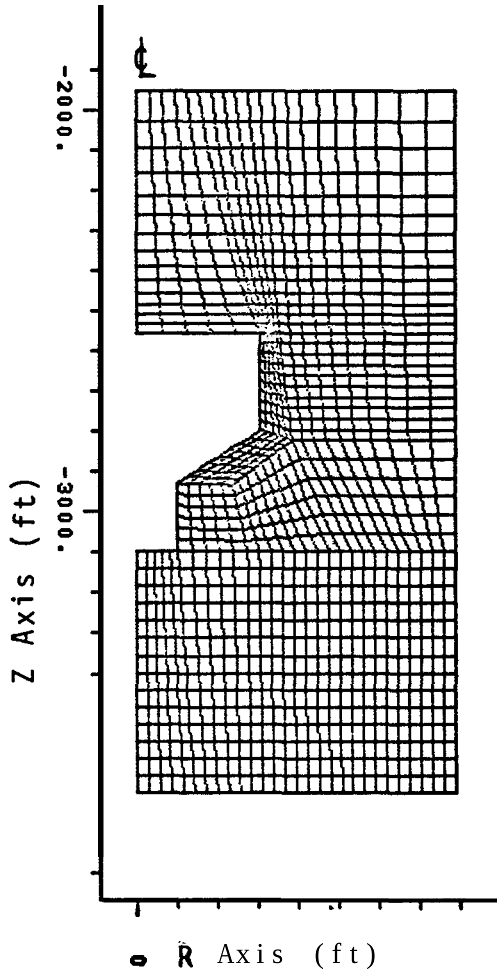

Figure 17

Axisymmetric Finite Element
Mesh of Bryan Mound Cavern Four

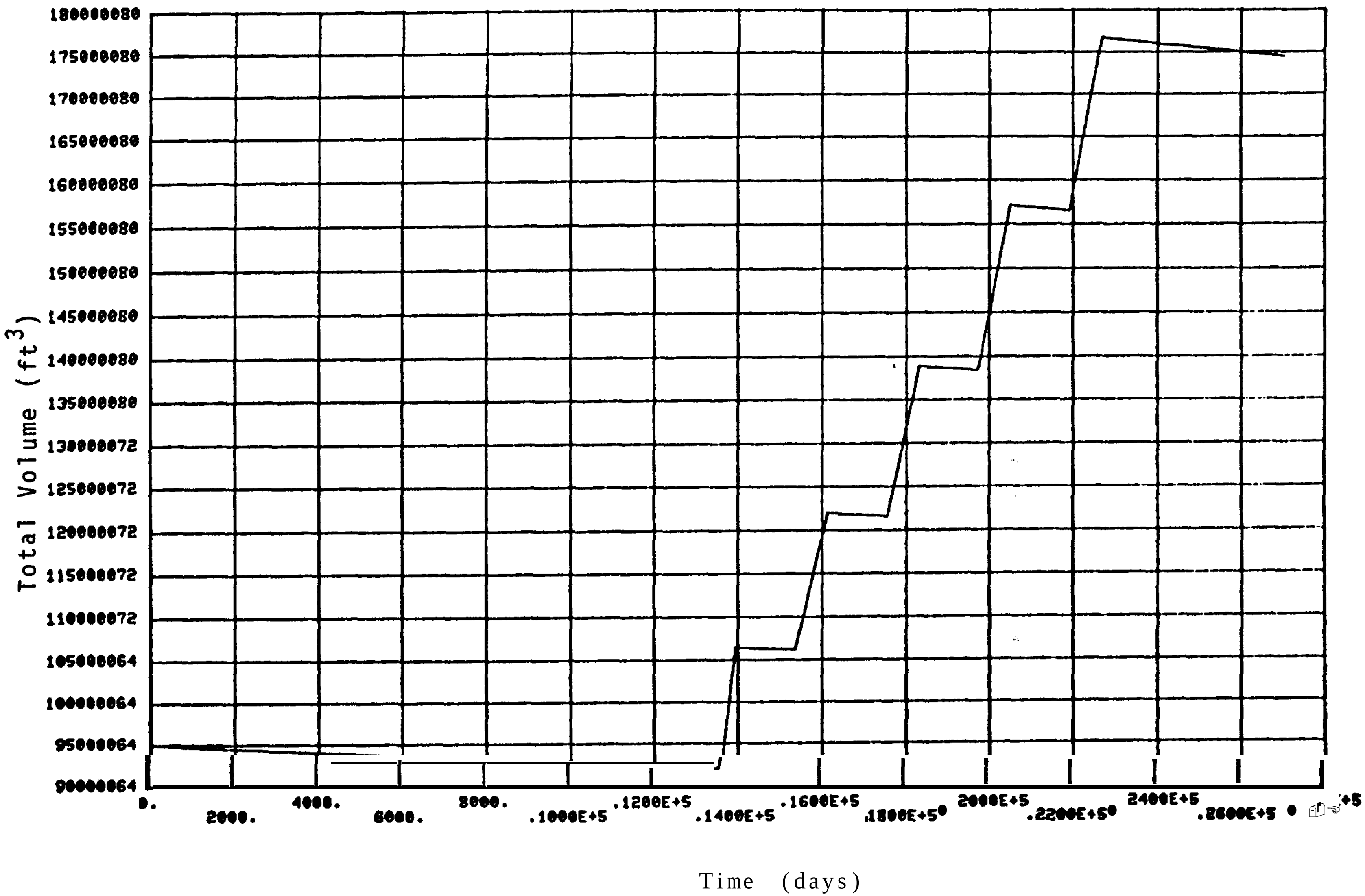

Figure 18
Volumetric Response of Cavern Four

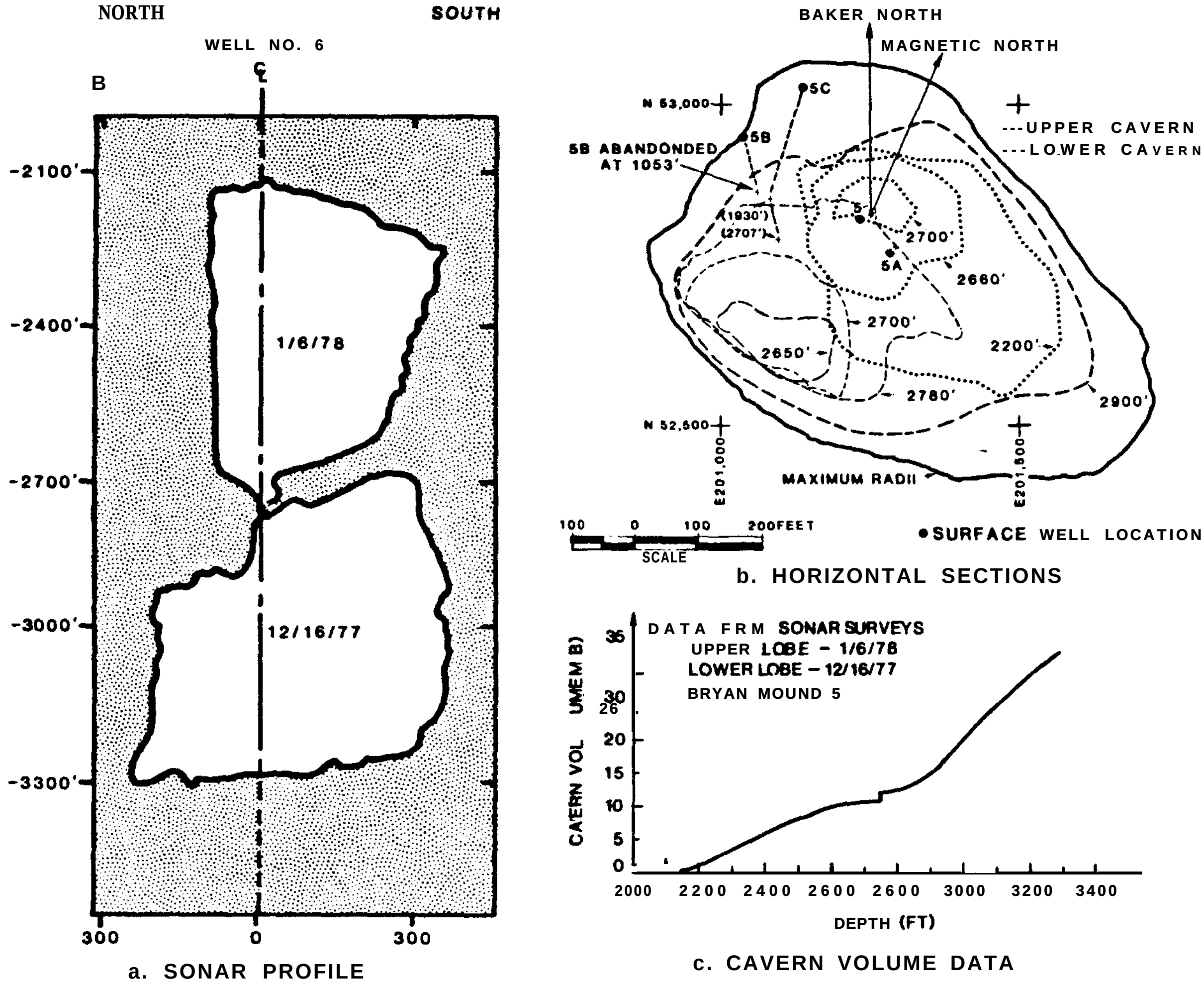

(After Hogan, 1980)

Figure 19
Bryan Mound Cavern Five

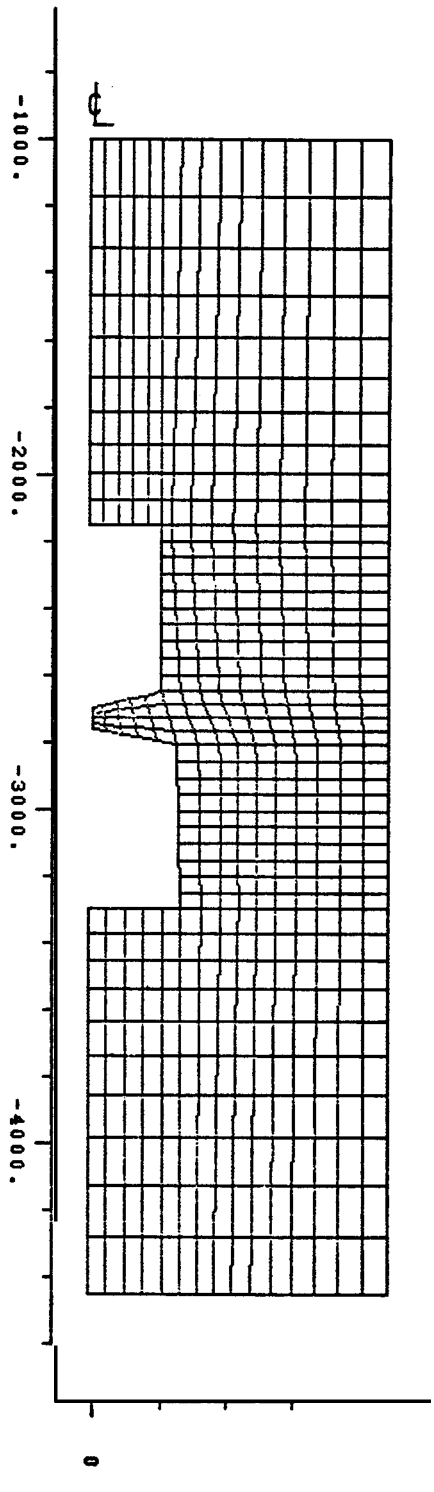

Figure 20

Axisymmetric Finite Element Mesh of Bryan Mound

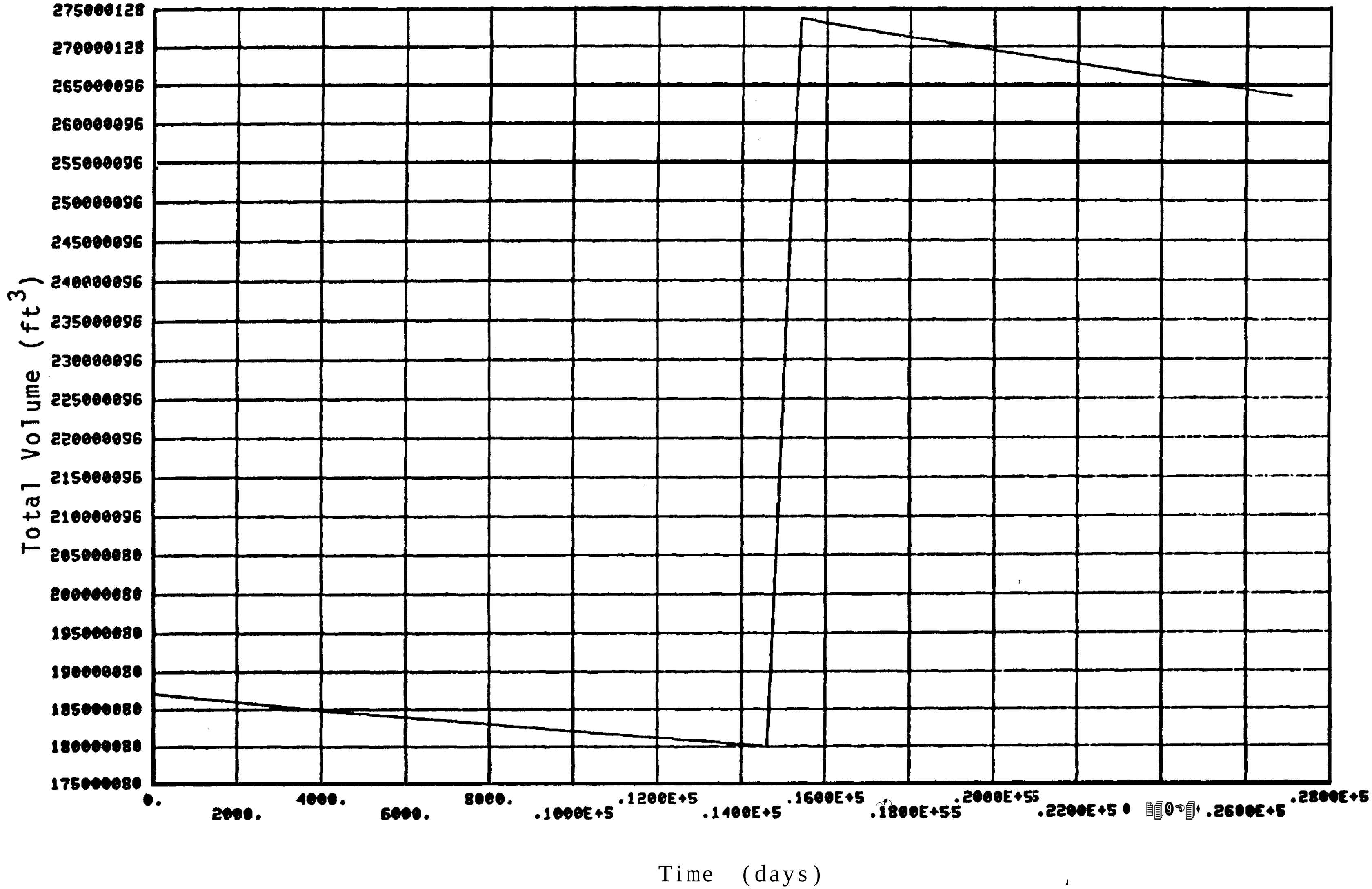

Figure 21

Volumetric Response of Cavern Five